



Published in final edited form as:

Cell Metab. 2008 November ; 8(5): 359–371. doi:10.1016/j.cmet.2008.09.008.

The glucagon receptor is required for the adaptive metabolic response to fasting

Christine Longuet[^], Elaine M. Sinclair[^], Adriano Maida[^], Laurie L. Baggio[^], Marlena Maziarz, Maureen J. Charron[#], and Daniel J. Drucker[^]

[^]*Department of Medicine, Samuel Lunenfeld Research Institute, Mount Sinai Hospital, University of Toronto, Toronto, Ontario, Canada, M5G 1X5*

[#]*Department of Biochemistry, Albert Einstein College of Medicine, Bronx, NY 10461, USA*

Abstract

Glucagon receptor (Gcgr) signaling maintains hepatic glucose production during the fasting state however the importance of the Gcgr for lipid metabolism is unclear. We show here that fasted Gcgr^{-/-} mice exhibit a significant increase in hepatic triglyceride secretion and fasting increases fatty acid oxidation (FAO) in wild type (WT) but not in Gcgr^{-/-} mice. Moreover fasting upregulated the expression of FAO-related hepatic mRNA transcripts in Gcgr^{+/+} but not in Gcgr^{-/-} mice. Exogenous glucagon administration reduced plasma triglycerides in WT mice, inhibited TG synthesis and secretion, and stimulated FA beta oxidation in Gcgr^{+/+} hepatocytes. The actions of glucagon on TG synthesis and FAO were abolished in PPAR α ^{-/-} hepatocytes. These findings demonstrate that the Gcgr receptor is required for control of lipid metabolism during the adaptive metabolic response to fasting

Introduction

Glucagon, a peptide of 29 amino acids released from pancreatic α -cells is the principal counterregulatory hormone that opposes the actions of insulin. Glucagon stimulates gluconeogenesis and promotes glycogenolysis leading to liberation of glucose from hepatocytes. These actions of glucagon are transduced via a G protein coupled receptor (GPCR) (the glucagon receptor or Gcgr), a member of the class II GPCR superfamily (Mayo et al., 2003). Glucagon action in the liver maintains normoglycemia in the fasted state via activation of a Gs protein, leading to the stimulation of adenylate cyclase activity, cAMP production, Epac, Torc2, PKA, and CREB activation (Jelinek et al., 1993; Koo et al., 2005; Wakelam et al., 1986). Glucagon also increases intracellular calcium in a phospholipase C dependent manner (Aromataris et al., 2006; Jelinek et al., 1993; Wakelam et al., 1986) and activates AMPK (Kimball et al., 2004) p38 MAPK (Cao et al., 2005; Chen et al., 1998) and JNK (Chen et al., 1998), through mechanisms that remain incompletely understood.

The control of glucagon secretion is dysregulated in human subjects with type II diabetes (T2DM) (Raskin and Unger, 1978; Unger, 1971), fostering efforts directed at suppression of

Correspondence to: Daniel J. Drucker.

Address correspondence to: Dr. Daniel J. Drucker Mount Sinai Hospital Samuel Lunenfeld Research Institute 600 University Avenue Room 975C Toronto Ontario Canada M5G 1X5 d.drucker@utoronto.ca.

Publisher's Disclaimer: This is a PDF file of an unedited manuscript that has been accepted for publication. As a service to our customers we are providing this early version of the manuscript. The manuscript will undergo copyediting, typesetting, and review of the resulting proof before it is published in its final citable form. Please note that during the production process errors may be discovered which could affect the content, and all legal disclaimers that apply to the journal pertain.

glucagon action for the treatment of T2DM. Indeed, diminution of glucagon action leads to reductions in blood glucose and improvement in glucose control in preclinical studies (Jiang and Zhang, 2003; Johnson et al., 1982; Unson et al., 1989). Moreover transient reduction of hepatic Gcgr expression in diabetic rodents was associated with significant improvements in glucose control (Liang et al., 2004; Sloop et al., 2004) and genetic inactivation of the Gcgr in mice is associated with mild fasting hypoglycemia, improved glucose tolerance and resistance to diet-induced obesity (Conarello et al., 2007; Gelling et al., 2003). Taken together, these studies confirm the importance of Gcgr signaling in the control of glucose homeostasis.

Improvement of metabolic control in the setting of glucose intolerance or experimental diabetes through attenuation of glucagon action has been associated with reduction in hepatic lipid accumulation and reduced levels of circulating triglycerides and free fatty acids (Conarello et al., 2007; Liang et al., 2004). Nevertheless, glucagon administration in the absence of diabetes produces potent hypolipemic actions (Bobe et al., 2003a; Eaton, 1973; Guettet et al., 1991) including decreased triglyceride (TG) and very low density lipoproteins (VLDL) release by the liver (Bobe et al., 2003a; Guettet et al., 1989), reduced levels of plasma cholesterol (Guettet et al., 1989; Guettet et al., 1988) and stimulation of hepatic free fatty acid (FFA) beta oxidation (Prip-Buus et al., 1990). Indeed, exogenous glucagon reduces liver triacylglycerol content and prevents the development of fatty liver in dairy cows (Bobe et al., 2006; Bobe et al., 2003b; Nafikov et al., 2006) whereas reduced glucagon action is associated with the development of fatty liver (Charbonneau et al., 2005a; Charbonneau et al., 2005b).

As the mechanisms linking Gcgr action to the control of lipid synthesis and/or FFA oxidation are poorly understood, we have now examined the importance of Gcgr signaling for lipid synthesis, secretion and oxidation in Gcgr^{+/+} and Gcgr^{-/-} mice. Our data provide new evidence implicating the Gcgr as an important integrator of metabolic signals converging on the peroxisome proliferator-activated receptor (PPAR α), leading to regulation of multiple components of hepatocyte lipid metabolism.

Results

The Gcgr is required for control of hepatic TG secretion

To assess the importance of Gcgr signaling for the regulation of plasma lipids, we measured circulating levels of TGs and FFA in Gcgr^{-/-} and Gcgr^{+/+} littermate control mice after fasting. No difference was observed in levels of plasma TGs and FFA in male Gcgr^{-/-} vs. Gcgr^{+/+} mice after 5 hours of fasting (Figure 1A, B) and TG levels were further reduced by 28% in Gcgr^{+/+} mice after 16h of fasting (Figure 1A). Unexpectedly, Gcgr^{-/-} mice exhibited a marked increase in plasma TGs and FFA after a 16 hr fast (Figure 1A, B; $p < 0.001$, and Figure S1A, B). Hepatic TG secretion, assessed following administration of triton WR1339 (Otway and Robinson, 1967; Scanu, 1965) was also significantly increased in male (Figure 1C; $p < 0.001$) and female Gcgr^{-/-} mice (Figure S1C). Consistent with findings in Gcgr^{-/-} mice, exogenous glucagon administration significantly decreased levels of plasma TGs and FFA in both male (Figure 1D, E) and female (Figure S1D, E) Gcgr^{+/+} mice. Similarly, glucagon inhibited hepatic TG secretion by 20% in male (Figure 1F; $p < 0.001$) and 30% in female (Figure S1F) Gcgr^{+/+} mice.

The effects of glucagon on plasma lipids were not secondary to stimulation of insulin secretion as levels of plasma insulin level and glucose were appropriately lower after fasting in both Gcgr^{+/+} and Gcgr^{-/-} mice (Figure S2A,B) and glucagon administration significantly increased glycemia (Figure S2D) but produced only modest increases in levels of plasma insulin (Figure S2C). Moreover, unlike the effects of exogenous glucagon (Figure 1F) which reduced TG secretion, insulin administration reduced glycemia (Figure S2F) but did not reduce TG secretion (Figure S2E). Similarly, while glucagon directly inhibited both TG synthesis and

secretion in murine hepatocytes in vitro, insulin exerted opposite stimulatory effects (Figure S2G, H). Therefore, the inhibitory effects of glucagon on TG synthesis and secretion are not likely mediated through stimulation of insulin secretion.

To elucidate the mechanisms important for glucagon action on lipid metabolism, we analysed p38 MAPK and AMPK, signaling molecules known to be important for the regulation of hepatic lipid metabolism. Glucagon rapidly and transiently stimulated both AMPK and p38 MAPK phosphorylation in murine hepatocytes (Figure 2A and 2B, respectively). Moreover, glucagon stimulated p38 MAPK activity and the p38 MAPK inhibitor SB203580 and the AMPK inhibitor (AMPKi) (but not the PKA inhibitor H89) prevented the glucagon-stimulated increase in p38 MAPK activity (Figure 2C).

Glucagon inhibits TG synthesis and secretion *via* distinct pathways

We next investigated the glucagon-regulated control of hepatocyte TG synthesis and secretion in murine hepatocytes. Glucagon had no effect on the intracellular levels of newly synthesized FFA in hepatocytes (Figure 3A), but significantly inhibited both TG synthesis (Figure 3B; $p < 0.001$) and secretion (Figure 3C; $p < 0.001$). The inhibitory actions of glucagon on both TG synthesis and secretion were not diminished by the PKA inhibitor H89 (Figure 3B, C respectively). In contrast, the glucagon-mediated inhibition of TG synthesis (Figure 3B), but not secretion (Figure 3C), was abolished following pharmacological inhibition of either p38 MAPK or AMPK. Similarly, glucagon was not able to inhibit TG synthesis, but still inhibited TG secretion (Figure S3B, C) following shRNA-mediated knockdown (by about 50%, Figure S3A) of p38MAPK and AMPK expression in hepatocytes.

FFA beta oxidation in liver homogenates from fasted and fed mice was monitored as conversion of 1-¹⁴C palmitate to ¹⁴CO₂ which increases linearly in hepatocytes as the rate of beta oxidation increases (Giordano et al., 2005). Fasting increased hepatic FFA oxidation in Gcgr^{+/+} mice (Figure 3D, 1.25 ± 0.05 $\mu\text{mol/g liver/hour}$ in fed vs 1.84 ± 0.1 $\mu\text{mol/g liver/hour}$ in fasted mice, $p < 0.01$). In contrast, FFA oxidation failed to increase and paradoxically decreased in fasting Gcgr^{-/-} mice (Figure 3D; 1.84 ± 0.1 $\mu\text{mol/g liver/hour}$ vs. 0.53 ± 0.08 $\mu\text{mol/g liver/hour}$ in fasted Gcgr^{+/+} vs. Gcgr^{-/-} mice, respectively $p < 0.001$). Moreover, FFA oxidation was also significantly lower in fed Gcgr^{-/-} mice (Figure 3D; $p < 0.05$, 1.25 ± 0.05 $\mu\text{mol/g liver/hour}$ in Gcgr^{+/+} vs. 0.92 ± 0.04 $\mu\text{mol/g liver/hour}$ in Gcgr^{-/-} mice, $p < 0.01$). The glucagon-stimulated increase in FFA beta oxidation was completely abolished by the p38 MAPK inhibitor SB203580 (Figure 3E) and no beta oxidation of fatty acids was detectable under basal or glucagon-stimulated conditions when hepatocytes were pre-treated with AMPKi (Figure 3E). Reduction of p38MAPK and AMPK expression using shRNA also abrogated the glucagons-stimulated increase in FAO oxidation (Figure S3D).

To determine whether the inhibitory effect of glucagon on TG synthesis may be indirect, perhaps reflecting reduced availability of FFA due to enhanced glucagon-stimulated fatty acid oxidation we examined whether inhibition of fatty acid oxidation results in increased levels of FFA available for TG synthesis. Hepatocytes were incubated with 1 μM etomoxir, an irreversible CPT1a antagonist known to inhibit FAO (Hiyoshi et al., 2003). Although glucagon alone had no significant effect on levels of FFAs in murine hepatocytes, glucagon stimulated a significant increase in levels of FFAs in hepatocytes treated with etomoxir (Figure 3F). Moreover, glucagon no longer inhibited TG synthesis but continued to inhibit TG secretion in the presence of etomoxir (Figure 3G, H). We conclude that glucagon inhibits TG synthesis by increasing FFA beta oxidation, thereby decreasing the availability of FFA for TG secretion.

To understand the mechanism(s) by which glucagon modulates the adaptation of hepatic lipid metabolism to fasting, we analysed hepatic gene expression profiles in fasted Gcgr^{+/+} vs. Gcgr^{-/-} mice. Fasting increased levels of mRNA transcripts for multiple genes important for

control of fatty acid beta oxidation in male and female *Gcgr*^{+/+} mice (Figure 4A and S4A). In contrast, levels of several mRNA transcripts of genes important for FAO were modestly increased in *Gcgr*^{-/-} mice (compare Fig 4A and 4B), and more prolonged fasting in *Gcgr*^{-/-} mice failed to upregulate levels of hepatic mRNA transcripts for *Facl2*, *Derc2*, *CPT2*, *Acadm*, *Ehadh*, *Hadha*, *Hadhb* (Figure 4B and S4B). Consistent with the importance of glucagon for changes in hepatic gene expression during fasting, exogenous administration of glucagon to WT mice produced a hepatic gene expression profile comparable to that detected during fasting, with significant increases in levels of mRNA transcripts for multiple genes involved in fatty acid beta oxidation (Figure 4C and S4C).

In contrast to the importance of the *Gcgr* for fasting-related changes in genes regulating FAO, the expression of genes regulating fatty acid synthesis was similarly decreased in *Gcgr*^{+/+} and *Gcgr*^{-/-} mice during fasting (Figure 4D, E and S4D, E). Furthermore, exogenous glucagon administration did not produce a reduction in levels of mRNA transcripts for the majority of genes regulating fatty acid synthesis (Figure 4F and S4F). These findings demonstrate that the *Gcgr* is essential for control of a genetic program regulating fatty acid beta oxidation, however *Gcgr* signaling is not essential for control of genes regulating fatty acid synthesis.

Glucagon stimulates PPAR α activity in a p38 MAPK and AMPK-dependent manner

As many of the glucagon-regulated genes important for fatty acid β -oxidation (Figure 4 and S4) are known targets of PPAR α (Patsouris et al., 2006), we assessed the role of PPAR α as a downstream target for glucagon action. Levels of liver PPAR α mRNA transcripts were comparable in fasted *Gcgr*^{-/-} vs *Gcgr*^{+/+} mice (Figure 5A) and exogenous glucagon produced a modest but nonsignificant increase in levels of PPAR α mRNA transcripts in WT mice (Figure 5B). Furthermore, hepatic PPAR α protein levels increased to similar levels during fasting in both *Gcgr*^{+/+} and *Gcgr*^{-/-} mice (Figure 5C). However, glucagon administration was associated with a marked redistribution in PPAR α immunoreactivity from the cytoplasm to hepatocyte nuclei (Figure 5D, lower panel). Furthermore, fasting was associated with nuclear translocation of PPAR α in liver of *Gcgr*^{+/+} mice, but not in *Gcgr*^{-/-} mice, in which considerable amounts of PPAR α remained in the cytoplasm (Figure 5E). Moreover fasting increased the binding of PPAR α to a Peroxisome Proliferator Response Element (PPRE) in EMSA studies using liver nuclear extracts from *Gcgr*^{+/+} mice but not in extracts from fasted *Gcgr*^{-/-} mice (Figure 5F).

To understand the mechanisms by which PPAR α remains in the cytoplasm under the fed state, we investigated the interaction of PPAR α with the chaperone protein HSP90. Under resting conditions PPAR α is bound to HSP90 in the cytoplasm and upon activation, dissociates from HSP90 and translocates to the nucleus to activate the transcription of target genes (Sumanasekera et al., 2003a; Sumanasekera et al., 2003b). Consistent with a role for HSP90 in the regulation of PPAR α activity, the HSP90 inhibitor 17DMAG significantly enhanced glucagon-induced PPAR α activity (Figure 5G). Furthermore, we observed a physical interaction of PPAR α with HSP90 in the cytoplasmic fraction prepared from primary murine hepatocyte cultures (Figure 5H). Moreover, the ability of glucagon to reduce the cytoplasmic localization and enhance the nuclear expression of phosphorylated PPAR α was markedly enhanced in the presence of 17DMAG (Figure 5H). Taken together, these data suggest that HSP90 is a chaperone for PPAR α in hepatocyte cytoplasm, and the HSP90-PPAR α interaction may regulate the extent of glucagon-dependent PPAR α activation in the nucleus.,

To assess whether the nuclear translocation of PPAR α was associated with an increase in PPAR α -dependent transcriptional activity, hepatocytes were transfected with a luciferase reporter gene containing 3 tandem copies of a PPRE. Glucagon increased PPRE-dependent luciferase activity by more than 4.5-fold in WT hepatocytes (Figure 5I, $p < 0.01$). As the PPRE integrates transcriptional responses from PPAR α , PPAR β and PPAR γ , we verified the importance of PPAR α as a downstream target of glucagon action using PPAR α knockout

(PPAR α ^{-/-}) mice. Indeed, the glucagon-stimulated induction of PPRE-dependent luciferase activity was substantially diminished in PPAR α ^{-/-} vs ^{+/+} hepatocytes (Figure 5I, $p < 0.01$). Hence, more than 70% of the glucagon-stimulated induction of PPRE transcriptional activity in hepatocytes is mediated by PPAR α . This increase in PPAR α activity upon glucagon stimulation was lost in Gcgr^{-/-} hepatocytes (Figure S5A). Furthermore, glucagon's effect on PPAR α activation in Gcgr^{+/+} hepatocytes was similar and non additive to the stimulation of PPAR α by the pharmacological activator WY14-643 (Figure S5B), and prevented by the PPAR α antagonist GW6471 (Figure S5C). The glucagon-stimulated PPAR α activation was abolished by the p38 MAPK inhibitor SB203580 (Figure 5J). Furthermore, fasting increases PPAR α interaction with p38MAPK in Gcgr^{+/+} mice, but not in Gcgr^{-/-} mice (Figure 5K), and this increased interaction is mimicked by glucagon (Figure 5L). These findings demonstrate that glucagon activates PPAR α in an AMPK- and p38 MAPK-dependent pathway.

We next examined the expression of other transcription factors involved in the regulation of hepatic lipid metabolism. The changes in expression of SREBP1, PGC1 α and ChREBP during fasting were not mimicked by glucagon administration, and/or were not regulated by glucagon or Gcgr genotype in a consistent manner in male and female mice (Figure S5D, E, F) whereas male and female mice display similar phenotypes in terms of plasma lipid levels (Figure 1 and S1) and gene expression (Figure 4 and S3) after fasting.

As FGF-21 and Acyl CoA Oxidase (ACO) have been identified as downstream targets of PPAR α capable of regulating fasting lipid metabolism (Badman et al., 2007; Inagaki et al., 2007), we assessed ACO and FGF-21 expression in Gcgr^{-/-} mice and in WT mice treated for 24h with glucagon. Both mRNA transcripts were induced in Gcgr^{+/+} liver after fasting (Figure S6A, C) however basal levels of both mRNAs were higher in Gcgr^{-/-} vs Gcgr^{+/+} mice and did not increase further with fasting (Figure S6A, C). Furthermore, glucagon had no effect on hepatic FGF-21 or ACO expression in WT mice (Figure S6B, D). Additionally, circulating levels of FGF-21 were not significantly different after fasting in Gcgr^{-/-} vs Gcgr^{+/+} mice, and glucagon administration had no effect on levels of circulating FGF-21 in Gcgr^{+/+} mice (Figure S6E, F). Hence, the effects of glucagon on hepatic lipid synthesis and secretion are not associated with corresponding changes in FGF-21 expression.

Glucagon modulates triglyceride synthesis and FFA beta oxidation in a PPAR α -dependent manner

We next investigated the role of PPAR α in the modulation of hepatic lipid metabolism by glucagon. No significant difference in FFA neosynthesis was observed in PPAR α ^{-/-} hepatocytes under basal or glucagon-stimulated conditions (Figure 6A). Although glucagon inhibited TG synthesis in ^{+/+} hepatocytes, glucagon failed to inhibit TG synthesis in PPAR α ^{-/-} hepatocytes (Figure 6B). In contrast the inhibitory effects of glucagon on TG secretion were preserved in PPAR α ^{-/-} hepatocytes (Figure 6C, 50.3% inhibition in PPAR α ^{+/+} vs 35.2% inhibition in PPAR α ^{-/-}). Similarly, the hypolipidemic effect of glucagon on levels of plasma FFA and TG as well as the glucagon-mediated inhibition of hepatic triglyceride secretion was preserved in PPAR α ^{-/-} mice (Figure S7A, B and C).

PPAR α was also essential for the ability of glucagon to regulate FAO, as glucagon stimulated ¹⁴CO₂ production in PPAR α ^{+/+} hepatocytes, but had no effect on FAO in PPAR α ^{-/-} mice (Figure 6D). Furthermore, in contrast to the glucagon-regulated FAO gene expression profile observed in ^{+/+} mice (Fig 4C), glucagon failed to modulate the expression of multiple genes involved in FFA beta oxidation in PPAR α ^{-/-} mice (Figure S7D). Finally, pharmacological activation of PPAR α in using fenofibrate restored normal levels of FFA beta oxidation in Gcgr^{-/-} liver homogenates (compare Fig. 3D vs 6E), increasing FFA beta oxidation by Gcgr^{-/-} liver homogenates to similar levels obtained with Gcgr^{+/+} liver homogenates. Taken together, these findings indicate that glucagon stimulates TG synthesis and FFA beta

oxidation in a PPAR α -dependent manner, and is required for the activation of PPAR α -dependent metabolic pathways during fasting.

Discussion

Glucagon levels are elevated in subjects with type 2 diabetes, and contribute to the development of excess hepatic glucose production and hyperglycaemia. Accordingly, Gcgr antagonists and antisense oligonucleotides (ASOs) directed against the Gcgr are being assessed for the treatment of T2DM, however, the consequences of blocking hepatic Gcgr signalling remain incompletely understood. Our data demonstrates that in the fasted state, glucagon action is essential for multiple pathways regulating lipid homeostasis. Furthermore, the actions of glucagon on lipid metabolism are mediated predominantly through AMPK, p38 MAPK and PPAR α -dependent mechanisms.

Analysis of lipid homeostasis in Gcgr $^{-/-}$ mice fasted for 5 hours did not reveal differences in levels of plasma TGs in Gcgr $^{-/-}$ vs. Gcgr $^{+/+}$ littermate controls, consistent with earlier findings (Gelling et al., 2003). In contrast a marked increase in plasma TGs was observed in Gcgr $^{-/-}$ mice after a more prolonged fast. Consistent with the improvement in hyperglycemia, levels of plasma and hepatic TGs were reduced in diabetic rodents following reduction of hepatic Gcgr expression; in contrast, the levels of plasma and liver TGs were paradoxically increased in control non-diabetic rats after ASO administration (Sloop et al., 2004). Similarly, treatment of db/db mice for 3 weeks with Gcgr ASOs resulted in a decrease in liver glycogen, but a significant increase in liver TGs in both the fasted and fed state (Liang et al., 2004). Hence, the available evidence suggests that the hepatic TG accumulation observed in fasted Gcgr $^{-/-}$ mice does not simply reflect abnormalities arising due to developmental loss of Gcgr signalling, but rather implicates a relationship linking diminished or absent Gcgr expression with the accumulation of hepatic TG.

FFA beta oxidation/ketogenesis is increased while lipogenesis is decreased during fasting, a state characterized by reduced levels of insulin and increased levels of glucagon and FFA. Studies using PPAR α $^{-/-}$ mice have demonstrated the central importance of PPAR α signalling pathways for the control of the adaptive metabolic response to fasting (Kersten et al., 1999). Remarkably Gcgr $^{-/-}$ mice exhibit increased hepatic TG secretion following fasting and enhanced susceptibility to hepatosteatosis following exposure to a high fat diet (Figure S8), features identical to those previously described in studies of PPAR α $^{-/-}$ mice (Kersten et al., 1999). Consistent with the importance of the Gcgr for the adaptive response to fasting, we observed increased expression of genes involved in beta oxidation and an increased capacity of liver to oxidize FFA during the fasted state in Gcgr $^{+/+}$ mice. However this gene expression signature was abolished in Gcgr $^{-/-}$ mice, which displayed defective oxidation of FFAs in both the fed and fasted state. Conversely, administration of glucagon further augmented the expression of genes regulating FAO and increased FFA oxidation in WT hepatocytes. Hence the results of experiments employing either loss or enhanced Gcgr signalling implicate an essential physiological role for Gcgr signalling in the control of a gene expression program linking fasting to enhanced fatty acid oxidation. Furthermore our data demonstrate that glucagon not only increases the capacity of hepatocytes to oxidize FFA, but also increases the availability of substrate for beta oxidation, as suggested by the significant increase in FFAs after glucagon stimulation when FFA beta oxidation is inhibited by etomoxir.

Glucagon is known to suppress lipogenesis in part via repression of sterol regulatory element binding protein-1c (SREBP-1c) expression (Foretz et al., 1999). Moreover exogenous glucagon stimulates cyclic AMP formation and cAMP response element-binding protein (CREB) activation, leading to control of a lipogenic gene expression program in a PPAR γ -dependent manner (Herzig et al., 2003). Recent studies have implicated a role for exogenous

glucagon in the control of lipogenesis via a p38 MAPK-dependent manner (Xiong et al., 2007). Inhibition of p38 leads to enhanced TG accumulation in fat-fed mice, together with increased expression of genes promoting hepatic lipogenesis. Conversely, exogenous glucagon reduced levels of SREBP-1c, SREBP-2, FAS, HMG CoA-R, and FFA mRNA transcripts in hepatocytes in a p38-dependent manner (Xiong et al., 2007). Although we also observed that glucagon reduced TG synthesis and fasting decreased expression of mRNA transcripts for lipogenic enzymes in Gcgr^{+/+} mice, loss of Gcgr signaling had no impact on the fasting-associated reduction in the lipogenic gene expression program. Hence, although glucagon may act pharmacologically to control lipogenesis through SREBP-1c and p38 MAPK, endogenous Gcgr signaling does not appear to be essential for suppression of a lipogenic gene expression program during fasting. Instead, glucagon directs FFA mobilized from TG stores toward beta oxidation rather than reesterification into triglyceride and secretion.

Classic concepts of glucose homeostasis implicate a central role for glucagon in the fasting state to promote enhanced gluconeogenesis and glycogenolysis. Levels of both circulating glucagon and hepatic PPAR α mRNA transcripts are increased by fasting and repressed by glucose (Lefebvre et al., 2006). Fasting is also associated with enhanced TG lipolysis, increased levels of FFA and increased hepatic fatty acid oxidation, thereby enhancing the availability of fuel substrates for use in peripheral tissues. Our current data extends physiological concepts of glucagon action by demonstrating that Gcgr signalling activates a p38MAPK- and PPAR α -dependent signaling network to enhance fatty acid oxidation. Moreover, disruption of endogenous Gcgr signalling impairs the control of fatty acid oxidation during fasting. These findings, summarized in Figure 7, taken together with our observations that Gcgr^{-/-} mice rapidly develop hepatosteatosis following high fat feeding (Figure S8) may have implications for therapeutic strategies designed to attenuate Gcgr signalling for the treatment of type 2 diabetes.

Material and Methods

Animals, treatments and reagents

Experiments were carried out using 8-12 week old global Gcgr^{-/-} mice and age and sex-matched littermate control mice in the C57BL/6 background (Gelling et al., 2003) for comparative analyses. Consistent with previous findings, we observed that food intake and body weight was similar in Gcgr^{-/-} and Gcgr^{+/+} littermate control mice (Gelling et al., 2003). For experiments employing PPAR α ^{-/-} mice (Jackson Laboratories, Bar Harbor, ME), age and sex-matched 129S1/SvImJ mice were used as WT controls (8-12 weeks of age) according to Jackson Laboratories recommendation. All mouse strains were maintained on standard rodent chow (unless otherwise indicated) under a normal 12h light- 12h dark cycle. All experiments were conducted according to protocols and guidelines approved by the Toronto General Hospital Animal Care Committee. To minimize the potential influence of circadian rhythms on experimental outcomes, standardized periods of fasting or experimental analyses were utilized. To test the effect of insulin, WT mice fasted for 5h were given 0.7 U/kg of human insulin (Novolin GE, Novo Nordisk) by intraperitoneal injection. To test the effect of repeated glucagon administration, mice were injected subcutaneously (sc) with glucagon (30 μ g/kg body weight in 500 μ L of 10% gelatine) or 10% gelatine alone, involving a total of 4 injections over a 24h period. Mice were euthanized 1 hour after the last injection, blood was obtained via cardiac puncture, and liver samples were collected, snap frozen in liquid nitrogen and stored at -80°C until further analysis. For acute glucagon injections, mice were fasted for 5 hours, then injected with glucagon (30 μ g/kg body weight via sc injection) in 500 μ L of 10% gelatin or with vehicle alone (10% gelatin). H89, SB 203580 and AMPKi were from Calbiochem, San Diego, CA and Etomoxir was from Sigma Aldrich, St. Louis, Mo.

In vivo hepatic TG secretion

After fasting and/or glucagon administration, mice were injected *via* the tail vein with Triton WR-1339 (0.5g/kg diluted 15% in PBS pH 7.4). Blood samples (50 μ L) were collected prior to IV injection and at 30 minutes, 1, 2 and 3h after injection.

Biochemical studies

Blood samples were collected by cardiac puncture or tail vein. For plasma preparation, blood samples were supplemented with trasyolol, EDTA and diprotin and centrifuged at 6,000 rpm at 4°C for 5 min. FFA and TGs were measured using colorimetric assays (NEFA kit and L-type TG kit-Wako chemicals (Richmond, VA)). Insulin levels were determined using a mouse ultra-sensitive insulin Elisa (Alpco Diagnostic). Blood glucose levels were measured using a Glucometer (Ascensia; Bayer HealthCare). FGF21 levels were assessed by radioimmunoassay (Phoenix Pharmaceuticals, Inc.).

Real-time PCR analysis of gene expression

RNA was extracted from liver using Trizol Reagent according to manufacturer instructions (Sigma-Aldrich, St. Louis, MO). Real-time quantitative PCR reactions were carried out using the Taqman® gene expression assay Universal PCR Master Mix (Applied Biosystems, Foster City, CA) and an ABI Prism 7900 Sequence Detection System (Applied Biosystems, Melbourne, Australia). Values for hepatocyte mRNA transcripts were normalized to the levels of GAPDH, as levels of GAPDH mRNA transcripts were not different between *Gcgr*^{+/+} and *Gcgr*^{-/-} mice and did not change following a 5 or 16h fast. Relative values for hepatocyte mRNA transcripts after glucagon administration were obtained by normalizing levels of mRNA transcripts to the levels of 18S rRNA in the same RNA samples, as glucagon administration increased levels of GAPDH mRNA transcripts.

Primary murine hepatocyte cultures

Murine hepatocytes were isolated as previously described (Flock et al., 2007), seeded in Primaria plates (BD Biosciences, Mississauga, ON) and allowed to attach for 2 to 4 hours prior to experimental treatments.

Lipid synthesis and secretion in hepatocytes

Cells were labelled with [³H]acetate (5 μ Ci/ml) in Williams E medium + 5% FBS for 16h and lipids were extracted twice with hexane:isopropanol 3:2 (v/v), the organic solvent was evaporated, and lipids were resuspended in hexane and spotted on a TLC plate. Neutral lipids were separated using ether:diethyl ether:glacial acetic acid 90:10:1 (v/v/v). Zones corresponding to the lipid standard were cut, mixed in scintillation cocktail overnight with gentle agitation, and counted on a Packard liquid scintillation counter. After lipid extraction, cells were digested in 1 ml of 50 mM NaOH and used for protein determination.

PPRE-luciferase activity

The PPAR-activated firefly luciferase reporter pHD(X3)Luc, obtained from Dr. J. Capone (McMaster University, Toronto, ON, Canada), contains three tandem copies of the PPRE from the rat enoyl-CoA hydratase/3-hydroxyacyl-CoA dehydrogenase gene upstream of a minimal promoter cloned into the plasmid pCPS-luc. (Zhang et al., 1993). After transfection of the reporter plasmid in Williams E media with lipofectamine 2000 at a ratio 1:3 (μ L lipofectamine 2000: μ g plasmid) for 5 hrs, hepatocytes (1 million per well in 6-well plates) were treated with 20 nM glucagon and/or 10 μ M SB203580. After 24 hours, cells were washed 3 times in ice-cold PBS and lysed in 250 μ L of harvest buffer (50 mM Tris/MES pH 7.8, 0.1% Triton X100, 1 mM DTT). Luciferase activity was determined using 200 μ L of cell lysate by adding 5 μ L

of luciferase cocktail (150 mM Tris/MES 1 M pH 7.8, 150 mM MgOAc, 40 mM ATP) and luminescence was assessed in a Berthold Tube Luminometer LB-9507. An aliquot of cell lysate was used for total protein determination.

Preparation of nuclear extracts and EMSA assays

Liver tissue (approximately 50 mg) was minced in 500 μ L of homogenisation buffer (10 mM Hepes pH 7.9, 10 mM KCl, 0.1 mM EDTA pH 7.4, 0.1 mM EGTA, 1 mM DTT, protease and phosphatase inhibitors). Homogenates were dounced 20 times (pestle B) and incubated on ice for 30 minutes prior to adding 6% of nonidet P40 10%. After an additional 30 minutes incubation on ice, homogenates were centrifuged for 1 minute at 13000 rpm at 4°C. The pellet containing nuclei was resuspended in 100 μ L of buffer containing 20 mM Hepes pH 7.9, 400 mM NaCl, 1 mM EDTA pH 7.4, 1 mM EGTA, 1 mM DTT, 5% glycerol, supplemented with protease and phosphatase inhibitors. Nuclei were incubated for 30 minutes on ice, and homogenates were vortexed every 10 minutes for 10 seconds. After a final 1 minute centrifugation at 13,000 rpm at 4°C, protein concentration determination in supernatant was performed as described previously (Rodriguez et al., 2000).

Immunohistochemistry

Primary hepatocytes were seeded in fibronectin-coated glass slide chambers. After 24h culture in Williams E media without serum but supplemented with 2 mM Glutamax, 100 U/ml penicillin and 100 μ g/mL streptomycin, cells were stimulated with 20 nM glucagon for 30 minutes, after which cells were fixed for 1h at room temperature in 4% formaldehyde. After 1h blocking in PBST + 10% donkey serum, cells were incubated overnight in a humidified chamber with anti-PPAR α antibody (Santa Cruz Biotechnology, Santa Cruz, CA) diluted 1/100 in PBS:1% Triton + 5% bovine serum albumin (BSA). Cells were then incubated for 1h at room temperature with Cy2-conjugated donkey anti-rabbit IgG, stained with 4',6-diamidino-2-phenylindole (DAPI) (1:50,000 in PBS for 15 minutes), and mounted using Dako fluorescent mounting medium (DakoCytomation Canada, Ontario, Canada). Cells were visualized using an Olympus FluoView FV1000 microscope and a 63X oil immersion objective, using sequential capture.

Western Blot analysis

Primary mouse hepatocytes were serum-starved for 24 hours in Williams E media supplemented with 2 mM GlutaMAX, 100 U/ml penicillin and 100 μ g/mL streptomycin, then stimulated with 20 nM glucagon in the presence or absence of signal transduction inhibitors added 30 minutes prior to glucagon. The experiment was terminated by transferring the plates onto ice and washing the cells with ice-cold PBS and protein samples were prepared as described (Koehler and Drucker, 2006). Antibodies against PPAR α (Fitzgerald Industries Intl, Concord, MA), phospho-p38 MAPK (Thr180/Tyr182), phospho-AMPK α (Thr172), total p38 MAPK, total AMPK, (Cell Signaling Technology, Beverly, MA) were used according to the manufacturer's instructions. Densitometry was performed on blots exposed on Biomax MR films (Eastman Kodak Co.) using a Hewlett-Packard ScanJet 3p scanner and NIH Image software.

p38 MAPK activity and protein analyses

Cells were lysed in 20 μ L of lysis buffer, and p38 MAPK assay was performed on 10 μ L of lysate using the TruLight p38 α Kinase Assay Kit (Calbiochem, La Jolla, CA), according to manufacturer instructions. Cell protein content was measured using BCA kit (Pierce, Rockford, IL), with BSA as the standard.

shRNA mediated knockdown of p38MAPK and AMPK

shRNA plasmid and Trans-lentiviral packaging system were purchased from Open Biosystem (Huntsville, AL). Lentivirus production and hepatocytes infection were performed according to manufacturer instructions. Lipid synthesis and FFA beta oxidation assays were done 36h after infection, as described above and below.

FFA beta oxidation in hepatocytes

FFA oxidation was assessed by measuring the production of $^{14}\text{CO}_2$ from $[1-^{14}\text{C}]$ palmitate. Briefly, hepatocytes (1 million in a 6 cm plate) were incubated for 24 h in serum-free Williams E medium containing 20 nM glucagon with or without signal transduction inhibitors. Plates were then washed with warm PBS and 2 mL of beta oxidation media (1 mM palmitate bound to fatty acid-free albumin at a molar ratio 5:1 in Williams E medium, 0.3 $\mu\text{Ci/mL}$ $1-^{14}\text{C}$ palmitate (Amersham Biosciences, Piscataway, NJ) with or without glucagon and/or inhibitors was added. Each petri dish was sealed with parafilm onto the inside of which a Whatman paper wet with 100 μl of phenylethylamine/methanol (1:1) was taped to trap the CO_2 produced during the incubation period. After a 2-h incubation period, 200 μl of H_2SO_4 (4 mol/l) was added to the cells, which were then further incubated for 1 h at 37°C . Finally, the seal was removed from each petri dish and the pieces of Whatman paper were transferred to scintillation vials for determination of radioactivity. An aliquot of media was counted to determine the total radioactivity.

FFA beta oxidation in liver homogenates

0.5 g of liver was manually homogenized using a Potter-Elvehjem homogenizer in 10 mL of ice-cold isolation buffer (220 mM mannitol, 70 mM sucrose, 2 mM HEPES, 0.1 mM EDTA pH 7.4). Aliquots of homogenate (300 μl) were added to 1.7 ml of reaction medium (50 mM sucrose, 150 mM Tris-HCl, 20 mM KH_2PO_4 , 10 mM $\text{MgCl}_2\cdot 6\text{H}_2\text{O}$, 2 mM EDTA, 1 mM L-carnitine, 0.2 mM CoA, 2 mM NAD, 0.1 mM malate, 10 mM ATP, 1 mM Palmitate complexed to fatty acid-free albumin at a 5:1 molar ratio in Williams E medium, 0.3 μCi of $[1-^{14}\text{C}]$ -palmitate (Amersham Biosciences), pH 7.4. Reactions performed in a sealed flask were allowed to proceed for 30 min in a shaking water bath at 37°C . Incubations were terminated by the addition of 1 ml of 3 M perchloric acid to the reaction medium to precipitate protein and non metabolized palmitate and then further incubated at room temperature for 2 h for collection of $^{14}\text{CO}_2$ into a suspended well containing 500 μl of ethanolamine. Blanks were prepared by acidification of the reaction medium immediately after the addition of the homogenate. Radioactivity in CO_2 was quantified by liquid scintillation spectrometry.

Statistical analysis

Statistical significance was assessed by one-way or two-way ANOVA using Bonferroni's multiple comparison post test and, where appropriate, by unpaired Student's t test using GraphPad Prism 4 (GraphPad Software, San Diego, CA). A p value of <0.05 was considered to be statistically significant.

Supplementary Material

Refer to Web version on PubMed Central for supplementary material.

Acknowledgements

CL was supported in part by a Research Fellowship Award from the Banting and Best Diabetes Centre and AM was supported in part by a Graduate Studentship Award from the Canadian Diabetes Association. The research was supported by an operating grant from the Canadian Institutes for Health Research MOP-10903 (DJD), by NIH grant

RO1 DK47425 to MC and the Canada Research Chairs Program (DJD). We thank Marc Angeli for helpful technical advice.

References

- Aromataris EC, Roberts ML, Barritt GJ, Rychkov GY. Glucagon activates Ca²⁺ and Cl⁻ channels in rat hepatocytes. *J Physiol* 2006;573:611–625. [PubMed: 16581855]
- Bobe G, Ametaj BN, Young JW, Anderson LL, Beitz DC. Exogenous glucagon effects on health and reproductive performance of lactating dairy cows with mild fatty liver. *Anim Reprod Sci.* 2006
- Bobe G, Ametaj BN, Young JW, Beitz DC. Effects of exogenous glucagon on lipids in lipoproteins and liver of lactating dairy cows. *J Dairy Sci* 2003a;86:2895–2903. [PubMed: 14507025]
- Bobe G, Ametaj BN, Young JW, Beitz DC. Potential treatment of fatty liver with 14-day subcutaneous injections of glucagon. *J Dairy Sci* 2003b;86:3138–3147. [PubMed: 14594232]
- Cao W, Collins QF, Becker TC, Robidoux J, Lupo EG Jr, Xiong Y, Daniel KW, Floering L, Collins S. p38 Mitogen-activated protein kinase plays a stimulatory role in hepatic gluconeogenesis. *J Biol Chem* 2005;280:42731–42737. [PubMed: 16272151]
- Charbonneau A, Couturier K, Gauthier MS, Lavoie JM. Evidence of hepatic glucagon resistance associated with hepatic steatosis: reversal effect of training. *Int J Sports Med* 2005a;26:432–441. [PubMed: 16037884]
- Charbonneau A, Melancon A, Lavoie C, Lavoie JM. Alterations in hepatic glucagon receptor density and in G α and G α 2 protein content with diet-induced hepatic steatosis: effects of acute exercise. *Am J Physiol Endocrinol Metab* 2005b;289:E8–14. [PubMed: 15687107]
- Chen J, Ishac EJ, Dent P, Kunos G, Gao B. Effects of ethanol on mitogen-activated protein kinase and stress-activated protein kinase cascades in normal and regenerating liver. *Biochem J* 1998;334(Pt 3): 669–676. [PubMed: 9729476]
- Conarello SL, Jiang G, Mu J, Li Z, Woods J, Zycband E, Ronan J, Liu F, Roy RS, Zhu L, Charron MJ, Zhang BB. Glucagon receptor knockout mice are resistant to diet-induced obesity and streptozotocin-mediated beta cell loss and hyperglycaemia. *Diabetologia* 2007;50:142–150. [PubMed: 17131145]
- Eaton RP. Hypolipemic action of glucagon in experimental endogenous lipemia in the rat. *J Lipid Res* 1973;14:312–318. [PubMed: 9704075]
- Flock G, Baggio LL, Longuet C, Drucker DJ. Incretin receptors for glucagon-like peptide 1 and glucose-dependent insulinotropic polypeptide are essential for the sustained metabolic actions of vildagliptin in mice. *Diabetes* 2007;56:3006–3013. [PubMed: 17717280]
- Foretz M, Pacot C, Dugail I, Lemarchand P, Guichard C, Le Liepvre X, Berthelie-Lubrano C, Spiegelman B, Kim JB, Ferre P, Foulfelle F. ADD1/SREBP-1c is required in the activation of hepatic lipogenic gene expression by glucose. *Mol Cell Biol* 1999;19:3760–3768. [PubMed: 10207099]
- Gelling RW, Du XQ, Dichmann DS, Romer J, Huang H, Cui L, Obici S, Tang B, Holst JJ, Fledelius C, Johansen PB, Rossetti L, Jelicks LA, Serup P, Nishimura E, Charron MJ. Lower blood glucose, hyperglucagonemia, and pancreatic {alpha} cell hyperplasia in glucagon receptor knockout mice. *Proc Natl Acad Sci U S A* 2003;100:1438–1443. [PubMed: 12552113]
- Giordano A, Calvani M, Petillo O, Grippo P, Tuccillo F, Melone MA, Bonelli P, Calarco A, Peluso G. tBid induces alterations of mitochondrial fatty acid oxidation flux by malonyl-CoA-independent inhibition of carnitine palmitoyltransferase-1. *Cell Death Differ* 2005;12:603–613. [PubMed: 15846373]
- Guettet C, Mathe D, Navarro N, Lecuyer B. Effects of chronic glucagon administration on rat lipoprotein composition. *Biochim Biophys Acta* 1989;1005:233–238. [PubMed: 2804052]
- Guettet C, Mathe D, Riottot M, Lutton C. Effects of chronic glucagon administration on cholesterol and bile acid metabolism. *Biochim Biophys Acta* 1988;963:215–223. [PubMed: 3058212]
- Guettet C, Rostaqui N, Mathe D, Lecuyer B, Navarro N, Jacotot B. Effect of chronic glucagon administration on lipoprotein composition in normally fed, fasted and cholesterol-fed rats. *Lipids* 1991;26:451–458. [PubMed: 1881241]
- Herzig S, Hedrick S, Morante I, Koo SH, Galimi F, Montminy M. CREB controls hepatic lipid metabolism through nuclear hormone receptor PPAR- γ . *Nature* 2003;426:190–193. [PubMed: 14614508]

- Hiyoshi H, Yanagimachi M, Ito M, Yasuda N, Okada T, Ikuta H, Shinmyo D, Tanaka K, Kurusu N, Yoshida I, Abe S, Saeki T, Tanaka H. Squalene synthase inhibitors suppress triglyceride biosynthesis through the farnesol pathway in rat hepatocytes. *J Lipid Res* 2003;44:128–135. [PubMed: 12518031]
- Jelinek LJ, Lok S, Rosenberg GB, Smith RA, Grant FJ, Biggs S, Bensch PA, Kuijper JL, Sheppard PO, Sprecher CA, O'Hara PJ, Foster D, Walker KM, Chen LHJ, Mckernan PA, Kindsvogel W. Expression cloning and signaling properties of the rat glucagon receptor. *Science* 1993;259:1614–1616. [PubMed: 8384375]
- Jiang G, Zhang BB. Glucagon and regulation of glucose metabolism. *Am J Physiol Endocrinol Metab* 2003;284:E671–678. [PubMed: 12626323]
- Johnson DG, Goebel CU, Hruba VJ, Bregman MD, Trivedi D. Hyperglycemia of diabetic rats decreased by a glucagon receptor antagonist. *Science* 1982;215:1115–1116. [PubMed: 6278587]
- Kersten S, Seydoux J, Peters JM, Gonzalez FJ, Desvergne B, Wahli W. Peroxisome proliferator-activated receptor alpha mediates the adaptive response to fasting. *J Clin Invest* 1999;103:1489–1498. [PubMed: 10359558]
- Kimball SR, Siegfried BA, Jefferson LS. Glucagon represses signaling through the mammalian target of rapamycin in rat liver by activating AMP-activated protein kinase. *J Biol Chem* 2004;279:54103–54109. [PubMed: 15494402]
- Koehler JA, Drucker DJ. Activation of GLP-1 receptor signaling does not modify the growth or apoptosis of human pancreatic cancer cells. *Diabetes* 2006;55:1369–1379. [PubMed: 16644694]
- Koo SH, Flechner L, Qi L, Zhang X, Srean RA, Jeffries S, Hedrick S, Xu W, Boussouar F, Brindle P, Takemori H, Montminy M. The CREB coactivator TORC2 is a key regulator of fasting glucose metabolism. *Nature* 2005;437:1109–1111. [PubMed: 16148943]
- Lefebvre P, Chinetti G, Fruchart JC, Staels B. Sorting out the roles of PPAR alpha in energy metabolism and vascular homeostasis. *J Clin Invest* 2006;116:571–580. [PubMed: 16511589]
- Liang Y, Osborne MC, Monia BP, Bhanot S, Gaarde WA, Reed C, She P, Jetton TL, Demarest KT. Reduction in Glucagon Receptor Expression by an Antisense Oligonucleotide Ameliorates Diabetic Syndrome in db/db Mice. *Diabetes* 2004;53:410–417. [PubMed: 14747292]
- Mayo KE, Miller LJ, Bataille D, Dalle S, Goke B, Thorens B, Drucker DJ. International Union of Pharmacology. XXXV. The Glucagon Receptor Family. *Pharmacol Rev* 2003;55:167–194. [PubMed: 12615957]
- Nafikov RA, Ametaj BN, Bobe G, Koehler KJ, Young JW, Beitz DC. Prevention of fatty liver in transition dairy cows by subcutaneous injections of glucagon. *J Dairy Sci* 2006;89:1533–1545. [PubMed: 16606724]
- Otway S, Robinson DS. The use of a non-ionic detergent (Triton WR 1339) to determine rates of triglyceride entry into the circulation of the rat under different physiological conditions. *J Physiol* 1967;190:321–332. [PubMed: 6049002]
- Prip-Buus C, Pegorier JP, Duee PH, Kohl C, Girard J. Evidence that the sensitivity of carnitine palmitoyltransferase I to inhibition by malonyl-CoA is an important site of regulation of hepatic fatty acid oxidation in the fetal and newborn rabbit. Perinatal development and effects of pancreatic hormones in cultured rabbit hepatocytes. *Biochem J* 1990;269:409–415. [PubMed: 2167069]
- Raskin P, Unger RH. Hyperglucagonemia and its suppression. Importance in the metabolic control of diabetes. *N Engl J Med* 1978;299:433–436. [PubMed: 683275]
- Rodriguez C, Noe V, Cabrero A, Ciudad CJ, Laguna JC. Differences in the formation of PPARalpha-RXR/acoPPRE complexes between responsive and nonresponsive species upon fibrate administration. *Mol Pharmacol* 2000;58:185–193. [PubMed: 10860941]
- Scanu AM. Factors affecting lipoprotein metabolism. *Adv Lipid Res* 1965;3:63–138. [PubMed: 5331623]
- Sloop KW, Cao JX, Siesky AM, Zhang HY, Bodenmiller DM, Cox AL, Jacobs SJ, Moyers JS, Owens RA, Showalter AD, Brenner MB, Raap A, Gromada J, Berridge BR, Monteith DK, Porksen N, McKay RA, Monia BP, Bhanot S, Watts LM, Michael MD. Hepatic and glucagon-like peptide-1-mediated reversal of diabetes by glucagon receptor antisense oligonucleotide inhibitors. *J Clin Invest* 2004;113:1571–1581. [PubMed: 15173883]
- Sumanasekera WK, Tien ES, Davis JW 2nd, Turpey R, Perdew GH, Vanden Heuvel JP. Heat shock protein-90 (Hsp90) acts as a repressor of peroxisome proliferator-activated receptor-alpha (PPARalpha) and PPARbeta activity. *Biochemistry* 2003a;42:10726–10735. [PubMed: 12962497]

- Sumanasekera WK, Tien ES, Turpey R, Vanden Heuvel JP, Perdew GH. Evidence that peroxisome proliferator-activated receptor alpha is complexed with the 90-kDa heat shock protein and the hepatitis virus B X-associated protein 2. *J Biol Chem* 2003b;278:4467–4473. [PubMed: 12482853]
- Unger RH. Glucagon physiology and pathophysiology. *N Engl J Med* 1971;285:443–449. [PubMed: 4997492]
- Unson CG, Gurzenda EM, Merrifield RB. Biological activities of des-His1[Glu9]glucagon amide, a glucagon antagonist. *Peptides* 1989;10:1171–1177. [PubMed: 2560175]
- Wakelam MJ, Murphy GJ, Hruby VJ, Houslay MD. Activation of two signal-transduction systems in hepatocytes by glucagon. *Nature* 1986;323:68–71. [PubMed: 3018586]
- Xiong Y, Collins QF, Jie A, Lupo E Jr, Liu HY, Liu D, Robidoux J, Liu Z, Cao W. p38 mitogen-activated protein kinase plays an inhibitory role in hepatic lipogenesis. *J Biol Chem* 2007;282:4975–4982. [PubMed: 17172644]
- Zhang B, Marcus SL, Miyata KS, Subramani S, Capone JP, Rachubinski RA. Characterization of protein-DNA interactions within the peroxisome proliferator-responsive element of the rat hydratase-dehydrogenase gene. *J Biol Chem* 1993;268:12939–12945. [PubMed: 8389766]

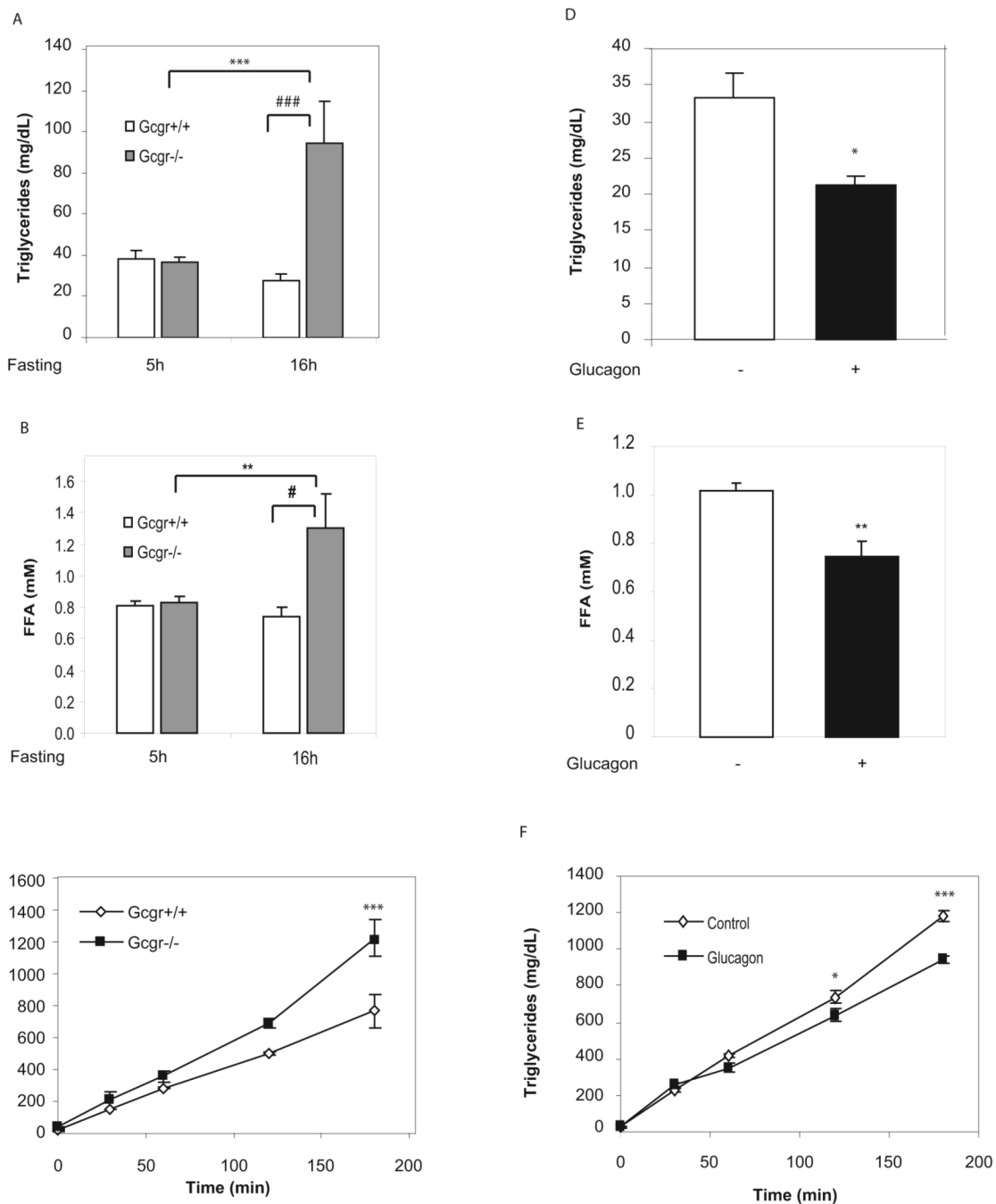


Figure 1. Glucagon decreases levels of plasma TGs and inhibits hepatic TG secretion *in vivo*
 TG (A and D) and FFA (B and E) levels were determined in plasma from Gcgr^{-/-} male mice and Gcgr^{+/+} littermate controls fasted for 5 or 16 hours (A, B) or from WT males treated with glucagon for 24h (30 ng/g body weight) as described in methods (D, E). C and F) Hepatic TG secretion was assessed indirectly by measurement of plasma TGs after intravenous injection of triton WR-1339 in Gcgr^{-/-} mice and +/+ littermate controls fasted for 16h (C) or WT males following a single glucagon injection, 30 ng/g BW as described in methods (F). Values are expressed as mean ± S.E.M. n = 4 to 11 mice per group. * = p<0.05; ** or # = p< 0.01; *** = p<0.001. ### = p< 0.001

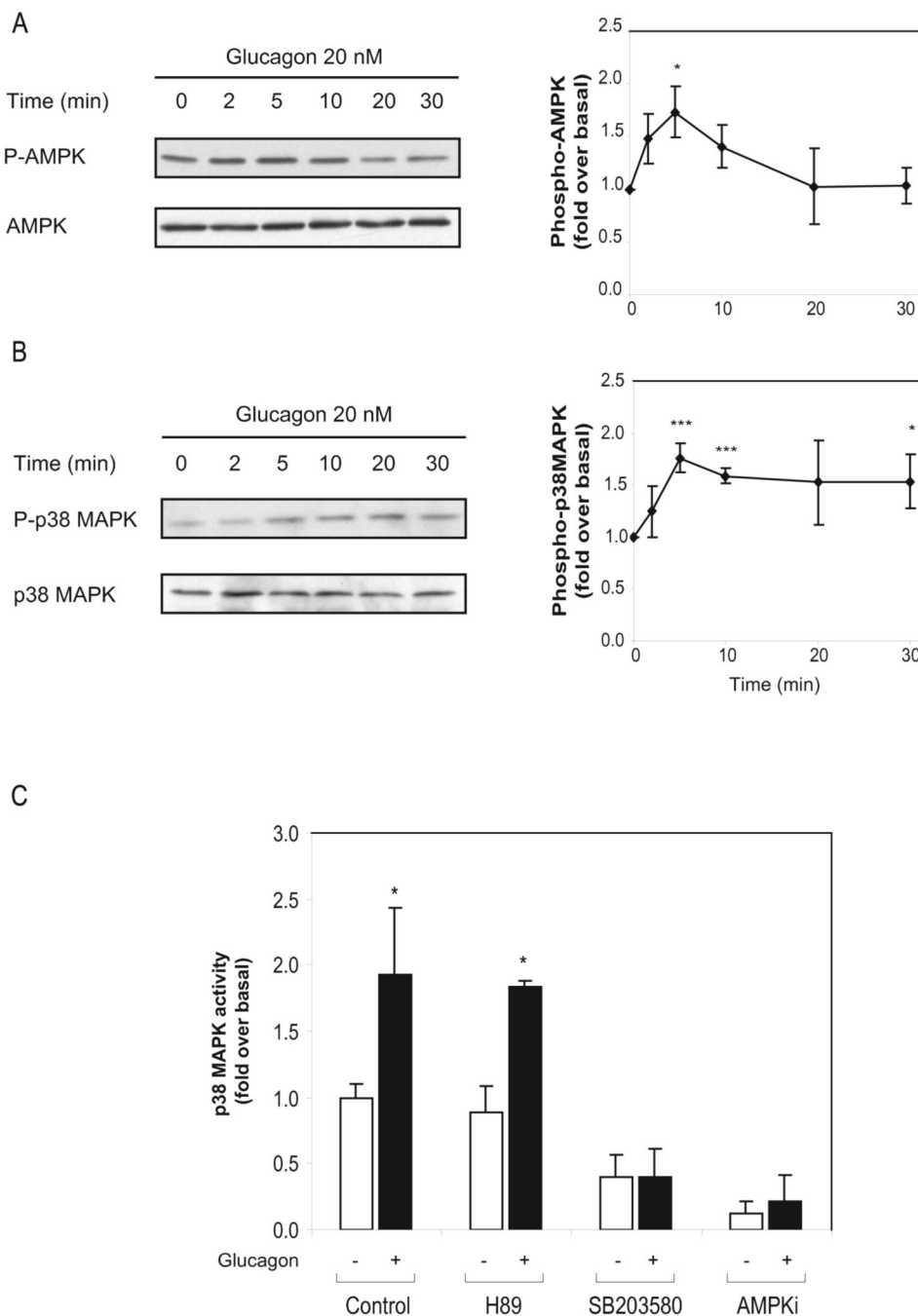


Figure 2. Glucagon activates p38 MAPK in an AMPK-dependent manner

A and B) Primary mouse hepatocytes from WT mice were cultured with or without 20 nM glucagon following which total cell lysates were prepared and subjected to Western blot analysis as described in Methods. * = $p < 0.05$, *** = $p < 0.001$ for levels of phosphorylated proteins in the presence or absence of glucagon. C) Mouse hepatocytes were cultured for 30 minutes with or without 20 nM glucagon in the presence or absence of 2 μ M H89, 10 μ M SB203580 or 20 μ M AMPKi. Data are mean \pm S.E.M., n = 6. * = $p < 0.01$ for values obtained in the presence or absence of glucagon

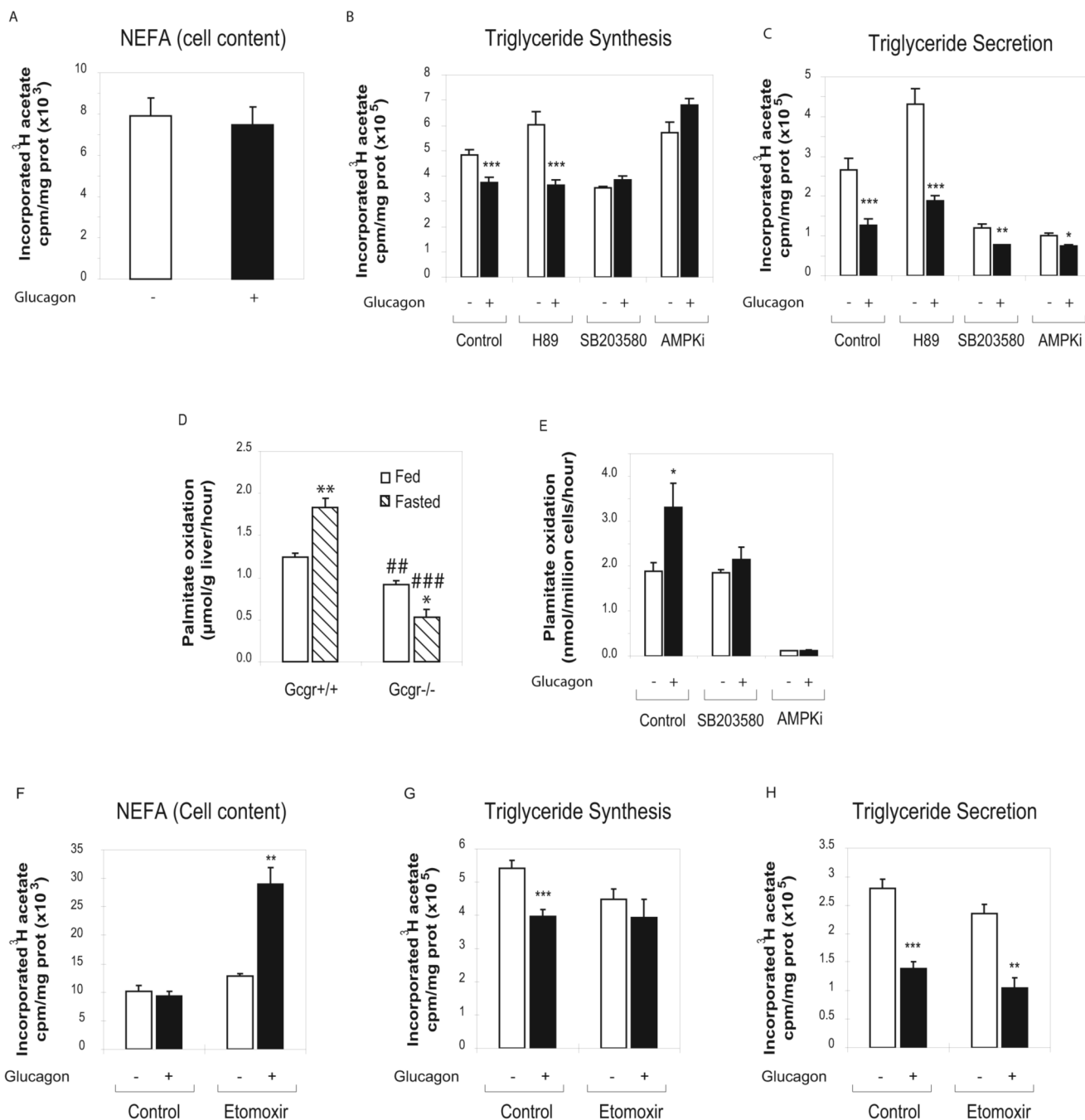


Figure 3. Glucagon modulates hepatic TG synthesis and secretion and FFA beta oxidation
 Lipid synthesis was assessed by measurement of FFAs and TGs in WT hepatocytes (A, B, C, F, G, H) treated for 16 hours with or without 20 nM glucagon in the presence or absence of 10 μM SB203580, 2 μM H89 or 20 μM AMPKi (A, B, C) or 1 μM etomoxir (F, G, H). Lipids were extracted from the media (secretion) or cells + media (synthesis), separated by TLC and quantified by scintillation counting. Data are mean \pm S.E.M. of 4 independent experiments. * = $p < 0.05$, ** = $p < 0.01$, *** = $p < 0.001$ for values obtained in the presence or absence of glucagon. Beta oxidation of [1- ^{14}C]-palmitate assessed in liver homogenates prepared from Gcgr $^{-/-}$ or littermate controls fed or fasted for 24 hours (D); in primary hepatocytes from WT mice treated with or without 20 nM glucagon for 24h in the presence or absence of 10 μM

SB203580 or 20 μ M AMPKi (E) as described in methods. Data are mean \pm S.E.M. of 6 independent experiments. * = $p < 0.05$, ** = $p < 0.01$ for fasted vs. the fed state in (D) and for vehicle vs. glucagon treated cells in (E); ## = $p < 0.01$, ### = $p < 0.001$ for Gcgr^{+/+} vs. Gcgr^{-/-} mice in D.

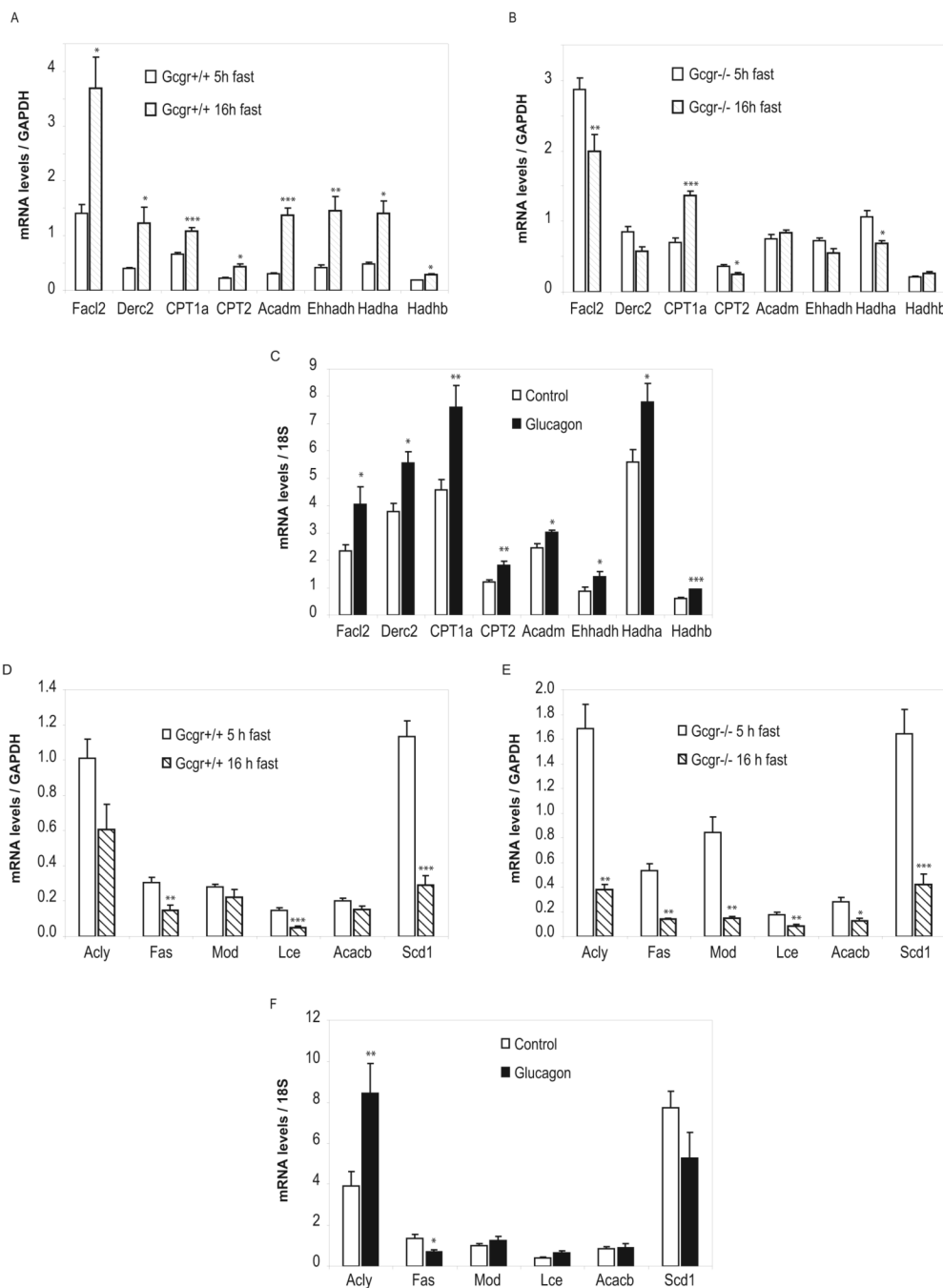
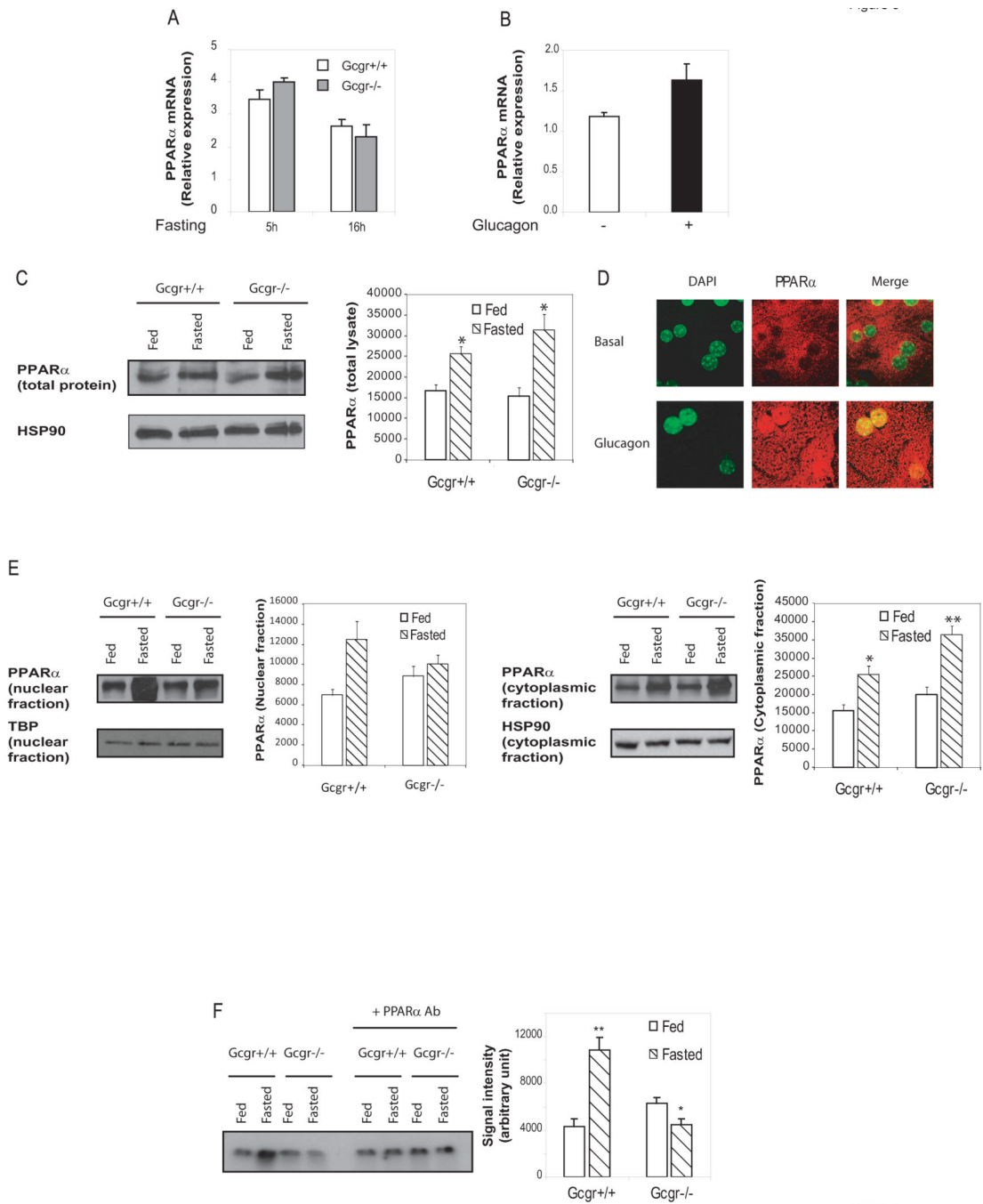


Figure 4. Hepatocyte gene expression profiles following fasting

Real time PCR was performed on RNA extracted from liver of male Gcgr^{-/-} and littermate control ^{+/+} mice after 5h or 16h fasting (A, B, D, E), and from WT males repeatedly injected with glucagon as described in methods (C, F). The relative level of mRNA transcripts detected was normalized to levels of GAPDH (A, B) or 18S (C). Data are mean ± S.E.M. (n = 4 to 11 mice in each group) and P values are assessed by one-way ANOVA test for comparison of gene expression * = p<0.05; ** = p< 0.01; *** = p<0.001 for differences in 5h vs. 16h fasted mice (A, B, D, E) or for vehicle vs. glucagon-treated mice (C, D). Facl2: Fatty Acid CoA ligase, long chain, 2; Derc2: 2-4-dienoyl-Coenzyme A reductase 2, peroxisomal; CPT1a: carnitine palmitoyltransferase 1A; CPT2: carnitine palmitoyltransferase 2; Acadm: acyl-Coenzyme A

dehydrogenase, medium chain; Ehhadh: enoyl-Coenzyme A, hydratase/3-hydroxyacyl Coenzyme A dehydrogenase (Peroxisomal bifunctional enzyme); Hadha: hydroxyacyl-Coenzyme A dehydrogenase/3-ketoacyl-Coenzyme A thiolase/enoyl-Coenzyme A hydratase (mitochondrial trifunctional protein), alpha subunit; Hadhb: hydroxyacyl-Coenzyme A dehydrogenase/3-ketoacyl-Coenzyme A thiolase/enoyl-Coenzyme A hydratase (mitochondrial trifunctional protein), beta subunit. Acly: ATP citrate lyase; Fas: fatty acid synthase; Mod: malic enzyme; Lce: long chain fatty acid elongase; Acacb: acetyl-Coenzyme A carboxylase beta; SCD1: stearoyl-Coenzyme A desaturase 1



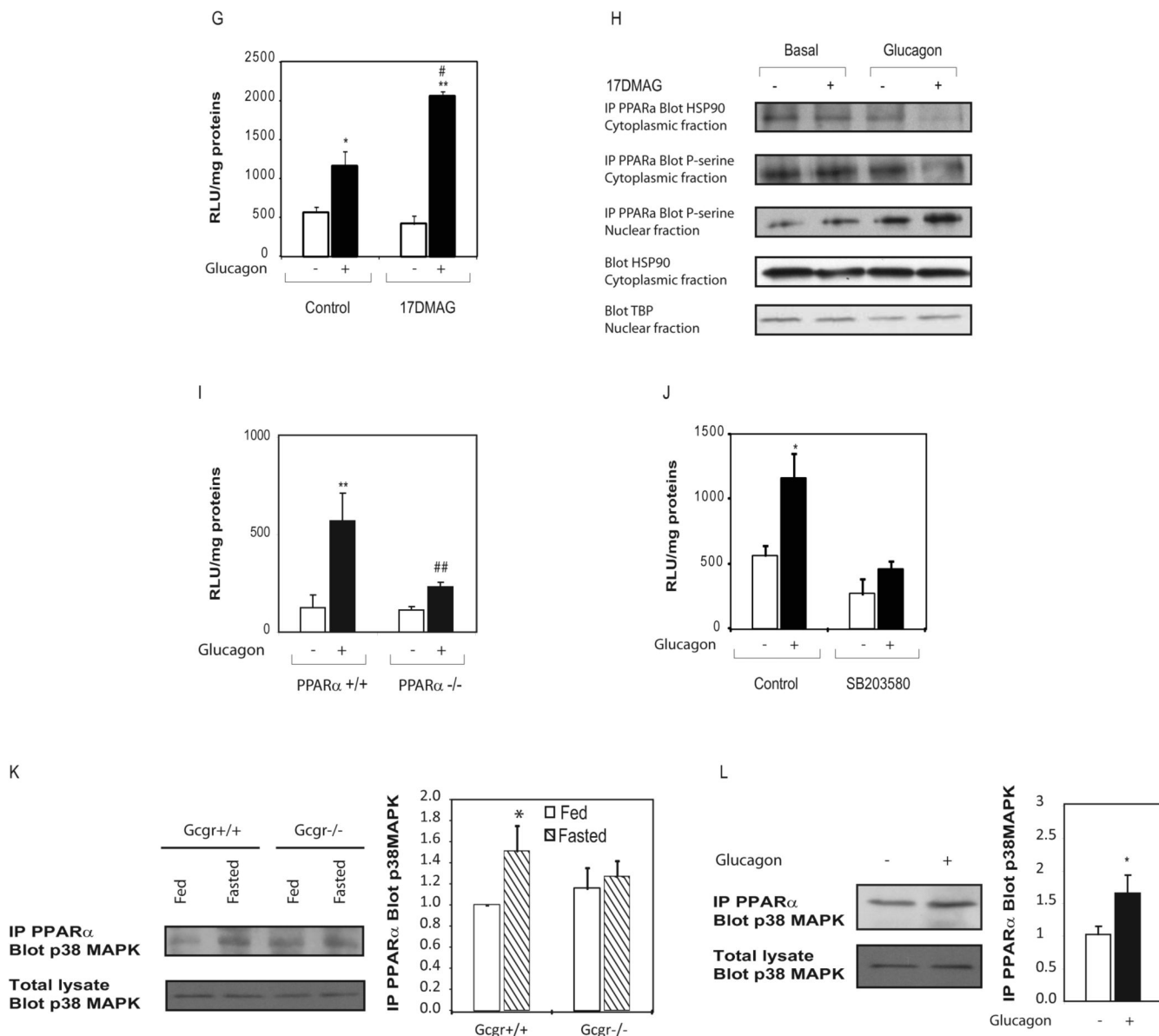


Figure 5. Glucagon activates PPAR α in a p38 MAPK- and AMPK-dependent manner
 Quantification of hepatic PPAR α mRNA transcripts from male Gcgr $^{-/-}$ vs. Gcgr $^{+/+}$ littermate controls fasted for 5 or 16 hours (A) or from WT male mice following chronic glucagon administration (B). Data are mean \pm S.E.M. (n = 4 to 11 mice in each group). C) Total liver lysates from Gcgr $^{+/+}$ and Gcgr $^{-/-}$ either fed or fasted for 16h were subjected to western blot analysis as described in methods. * = p<0.05 for levels of proteins in the fed vs fasted state. Data are mean \pm S.E.M. (n = 4 mice in each group) D) Immunofluorescence staining of PPAR α protein in primary mouse hepatocytes cultured in vitro with or without 20 nM glucagon for 30 minutes. E) Nuclear (left panel) and cytoplasmic (right panel) fractions were purified from liver of Gcgr $^{+/+}$ and Gcgr $^{-/-}$ either fed or fasted for 16h and nuclear proteins were analyzed by Western blotting as described in methods. HSP90 (cytoplasmic fraction) and TATA Binding Protein (TBP) (nuclear fraction) were used as loading controls. No HSP90 was detectable in the nuclear fraction, and no TBP was detectable in cytoplasmic fraction (data not shown)* = p<0.05 for levels of proteins in the fed vs fasted state. Data are mean \pm S.E.M.

(n = 4 mice in each group) F) Gel shift motility assay was performed using nuclear extract from liver of Gcgr^{-/-} mice or littermate controls either fed or fasted for 16h, incubated with a radiolabelled ACO-probe as described in methods. Data are mean ± S.E.M. of 4 independent experiments. * = p<0.05 ** = p<0.01 for fed vs. fasted mice. G I and J) Primary hepatocytes prepared from PPAR α ^{+/+} or PPAR α ^{-/-} mice (I) or from WT mice (G and J) were transfected with the PPAR-responsive luciferase reporter pHD(X3)Luc, and further incubated for 24 hours with vehicle alone or 20 nM glucagon, with or without 10 μ M SB203580 (J) or with or without 500 nM 17DMAG (G) Data are mean ± S.E.M. of 3 experiments. ** = p<0.01 for control vs. glucagon-treated cells; ## = p<0.01 for glucagon-stimulated PPAR α ^{+/+} vs PPAR^{-/-} hepatocytes or glucagon treatment in control vs. SB203580-treated hepatocytes. H) After 30 min stimulation with 20 nM glucagon with or without 500 nM 17 DMAG, nuclear and cytoplasmic fractions were purified from primary WT hepatocytes. PPAR α was immunoprecipitated in each fraction and blotted for HSP90 (upper panel) or phosphoserine (lower panels) HSP90 (cytoplasmic fraction) and TATA Binding Protein (TBP) (nuclear fraction) were used as loading controls. K and L) PPAR α was immunoprecipitated from liver lysate prepared from Gcgr^{+/+} and Gcgr^{-/-} fed or fasted for 16h (K), or from WT mice injected with glucagon (L), then subjected to western blot analysis using an anti-p38 MAPK antibody. Total p38MAPK in total lysate is shown as a loading control.

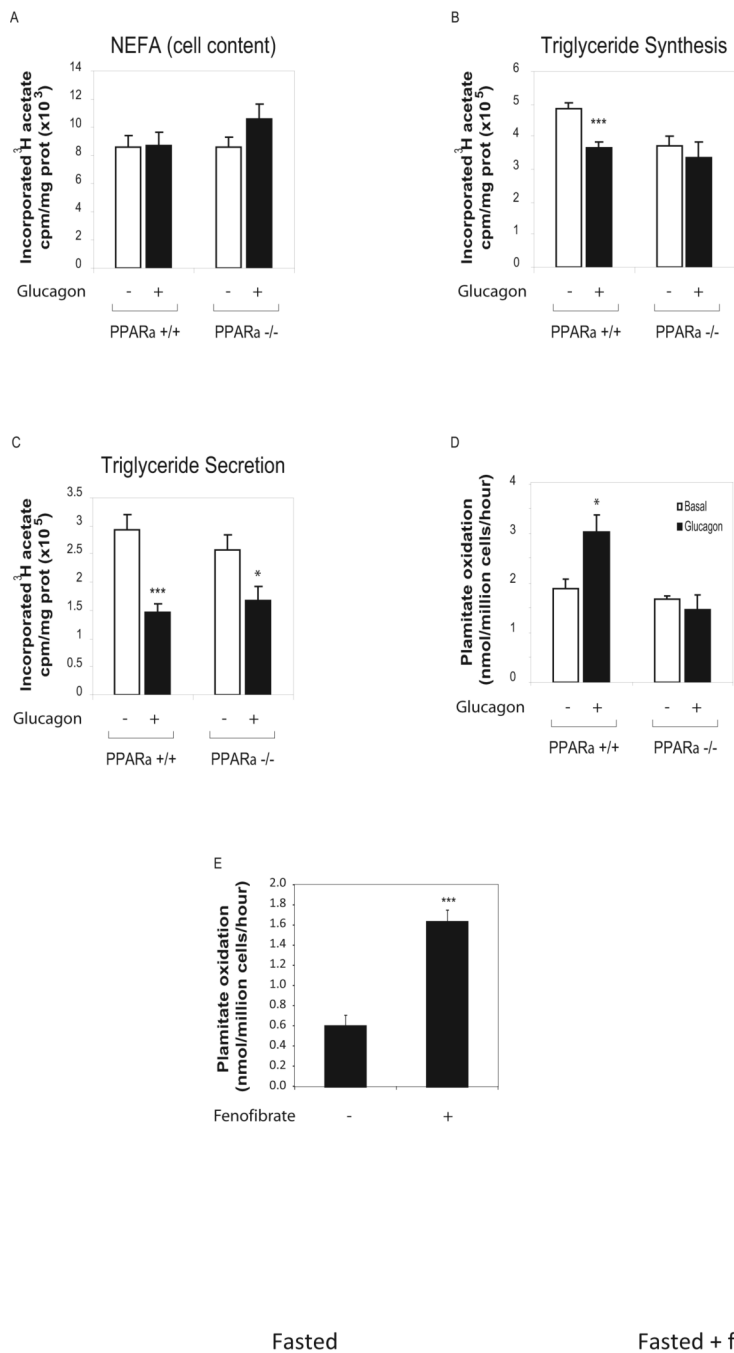


Figure 6. Glucagon increases FAO and inhibits TG synthesis in a PPAR α -dependent manner
 A, B and C) Lipid synthesis was assessed by measurement of FFAs and TGs in hepatocytes from WT and PPAR α -/- mice treated for 16 hours with or without 20 nM glucagon. Lipids were extracted from the media (secretion) or cells + media (synthesis), separated by TLC and quantified by scintillation counting. Data are mean \pm S.E.M. of 4 independent experiments. * = p<0.05, *** = p<.001 for values obtained in the presence or absence of glucagon. D) Beta oxidation of [¹⁴C]- palmitate assessed in primary hepatocytes from WT or PPAR α -/- mice and treated with or without 20 nM glucagon for 24h as described in methods. E) Beta oxidation of [1-¹⁴C]-palmitate assessed in liver homogenates prepared from Gcgr-/- fasted for 24 hours with or without fenofibrate administration during fasting as described in methods. Data are

mean \pm S.E.M. of 6 independent experiments. * = $p < 0.05$ for vehicle vs. glucagon treated cells in (C)

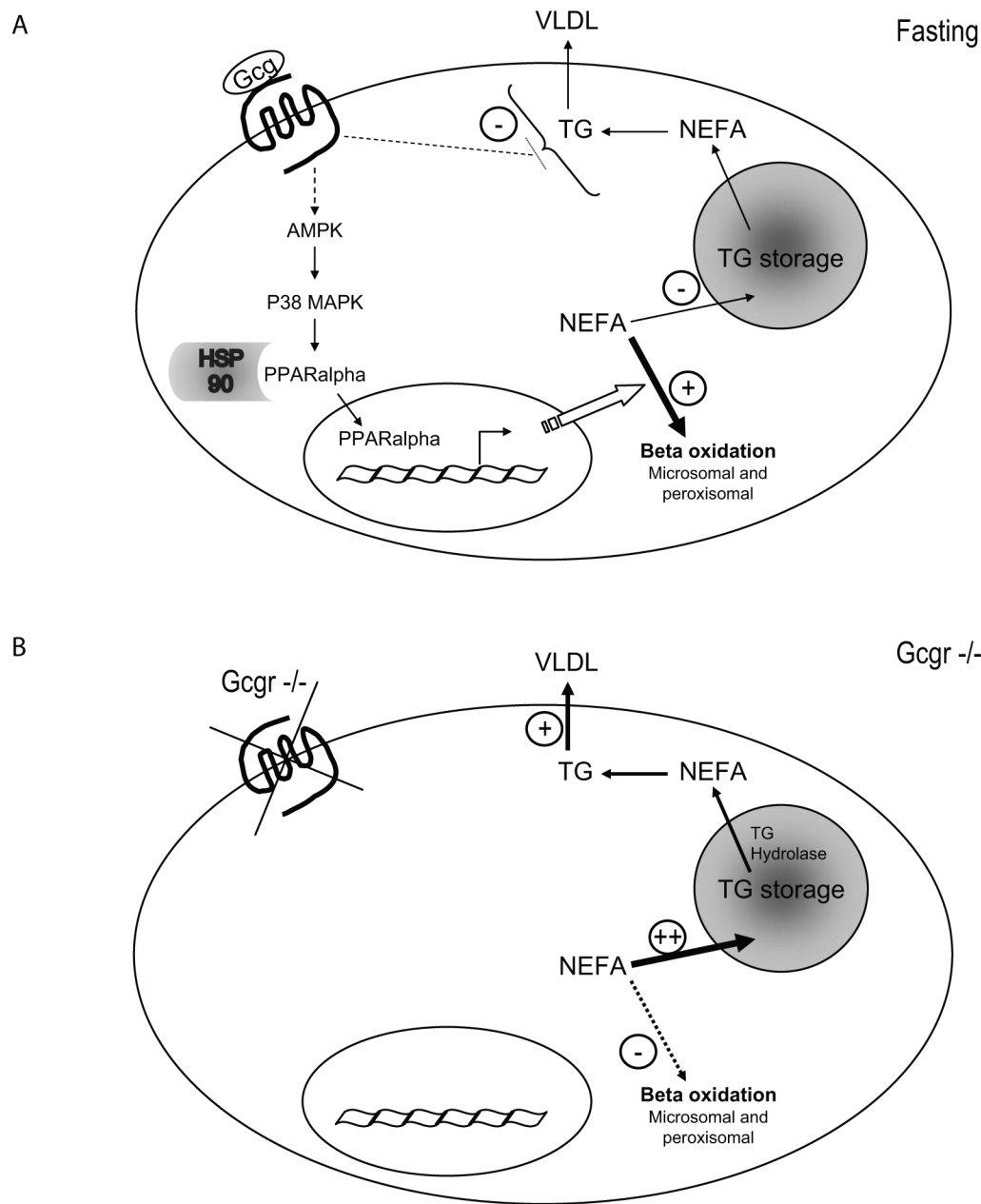


Figure 7. The effects of glucagon on hepatic lipid metabolism

A) During fasting, glucagon sequentially activates AMPK and p38 MAPK, leading to the dissociation from HSP90 and nuclear translocation and transcriptional activation of PPAR α , which then stimulates the transcription of genes involved in FFA beta oxidation. Glucagon increases the ratio of FFAs targeted to beta oxidation vs TG synthesis, resulting in decreased TG storage. Glucagon also decreases TG secretion, independently of PPAR α activation and FFA beta oxidation. B) In the absence of glucagon signalling in Gcgr $^{-/-}$ mice, FFA beta oxidation is decreased, leading to increased TG storage/secretion.